Next-to-Next-to-Leading-Order QCD Prediction for the Pion Form Factor

Based on arXiv: 2411.03658 with Y.JI, J.WANG, Y.F.WANG, Y.M.WANG, H.X.YU

Bo-Xuan Shi

The 7th Workshop on Heavy Flavor Physics and Quantum Chromodynamics

Nankai University, April 20, 2025

Motivations & Background

- Process $\pi^+\gamma^* \to \pi^+$ with space-like momentum transfer $Q^2 \equiv -(p'-p)^2$ is theoretically clean.

$$\langle \pi^+(p')|j_\mu^{\mathrm{em}}(0)|\pi^+(p)\rangle = F_\pi(Q^2)\,(p+p')_\mu$$

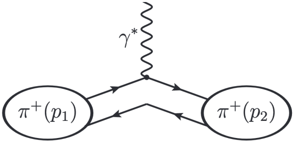

- Investigating the hard-collinear factorization properties at leading power.
- Key targets for the forthcoming EIC experiments at BNL with high precision.

  R. Abdul Khalek et al., Nucl. Phys. A 1026, 122447 (2022), arXiv:2103.05419 [physics.ins-det].

- Next-to-leading order calculation:
  - R. D. Field et al (1981), F.-M. Dittes et al (1981), R. S. Khalmuradov et al (1985) $\Leftarrow$ wrong hard kernel
  - M. H. Sarmadi (1982), E. Braaten et al (1987) $\Leftarrow$ violate universality of LCDA
  - Melic et al (1999) $\Leftarrow$ covariant trace prescription
- Next-to-next-leading order calculation:
  - L.-B. Chen, W. Chen, F. Feng, and Y. Jia, Phys. Rev. Lett. 132, 201901 (2024), arXiv:2312.17228 [hep-ph] $\Leftarrow$ covariant trace prescription
- In this work, we calculate the pion electromagnetic form factor (EMFF) within a rigorous factorization framework by including the evanescent contributions.

Definition & Kinematics

- (Space-like) Pion EMFF can be defined as

$$\langle \pi^+(p')|j_\mu^{\text{em}}(0)|\pi^+(p)\rangle = \underbrace{F_\pi(Q^2)}_{\text{real valued}}\,(p+p')_\mu + \underbrace{\tilde{F}_\pi(Q^2)\,(p-p')_\mu}_{\text{vanished due to current conservation}} \tag{1}$$

$$j_\mu^{\text{em}}(x) = \sum_q e_q\,\bar{q}(x)\gamma_\mu q(x)\,. \tag{2}$$

- Isospin symmetry indicates

$$F_{\pi^-}(Q^2) = -F_\pi(Q^2), \qquad F_{\pi^0}(Q^2) = 0. \tag{3}$$

- Electric charge conservation indicates

$$F_\pi(0) = 1. \tag{4}$$

- For large Q^2, we introduce two light-cone momentum n, $\bar{n}$ $(n\cdot\bar{n} = 2)$

$$p_\mu = (n\cdot p)\frac{\bar{n}_\mu}{2}, \qquad p'_\mu = (\bar{n}\cdot p')\frac{n_\mu}{2}, \qquad n\cdot p \sim \bar{n}\cdot p' \sim \mathcal{O}(\sqrt{Q^2}) \tag{5}$$

Factorization

- Leading power factorization

$$F_\pi(Q^2) = (e_u - e_d)\frac{4\pi\alpha_s(\nu)}{Q^2} f_\pi^2 \int dx \int dy\, T_1(x, y, Q^2, \nu, \mu)\, \phi_\pi(x, \mu)\, \phi_\pi(y, \mu)\,, \tag{6}$$

where x, y are momentum fraction carried by u-quark.

- Non-perturbative quantity — leading-twist pion LCDA ϕ_π

$$\langle \pi^+(p')|\bar{u}(\tau\,\bar{n})\,[\tau\,\bar{n}, 0]\,\gamma_\mu\,\gamma_5\,d(0)|0\rangle = -i\,f_\pi\,p'_\mu \int_0^1 dx\, e^{ix\,\tau\,\bar{n}\cdot p'}\,\phi_\pi(x, \mu)\,, \tag{7}$$

- Hard kernel $T_1(x, y, Q^2, \nu, \mu)$ can be extracted from correlator perturbatively

$$\begin{aligned}\Pi_\mu =& \langle u(p_1')\,\bar{d}(p_2')|j_\mu^{\text{em}}(0)|u(p_1)\,\bar{d}(p_2)\rangle\,,\\ =&(p+p')_\mu \left[(e_u - e_d)\,\frac{4\pi\alpha_s}{Q^4}\sum_k T_k \otimes \langle \mathcal{O}_k\rangle\right].\end{aligned}$$

$$T_k = \sum_{\ell=0}^{\infty}\left(\frac{\alpha_s}{4\pi}\right)^{\ell} T_k^{(\ell)}. \tag{8}$$

Operator basis

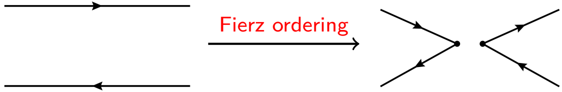

$$\Pi_\mu = (p+p')_\mu \left[(e_u - e_d) \frac{4\pi\alpha_s}{Q^4} \sum_k T_k \otimes \langle \mathcal{O}_k \rangle \right], \tag{9}$$

- Operator basis is

$$\begin{aligned} \mathcal{O}_1 &= [\bar{\chi}_u \not{\bar{n}} \gamma_5 \chi_d] [\bar{\xi}_d \not{n} \gamma_5 \xi_u], \\ \mathcal{O}_2 &= [\bar{\chi}_u \gamma_{\perp\alpha} \xi_u] [\bar{\xi}_d \gamma_\perp^\alpha \chi_d] - \frac{1}{4} \mathcal{O}_1, \\ \mathcal{O}_3 &= [\bar{\chi}_u \gamma_{\perp\alpha} \gamma_{\perp\mu_1} \gamma_{\perp\mu_2} \xi_u] [\bar{\xi}_d \gamma_\perp^\alpha \gamma_\perp^{\mu_2} \gamma_\perp^{\mu_1} \chi_d]. \end{aligned} \tag{10}$$

- $\mathcal{O}_1$ is physical and $\mathcal{O}_{2,3}$ are evanescent, namely, vanish under $d \to 4$.
- The evanescent operators originate from the infinite-dimensional Dirac algebras under dimensional regularization.
- At NLO, evanescent operators can contribute to constant terms, while at NNLO, they can contribute to both $1/\epsilon$ divergences and constant terms.
- The number of evanescent operators grows as the loop order increases.

Matching & Master formulae

- Matching two formulae of Π_μ

$$\Pi_\mu = (p+p')_\mu \ (e_u - e_d) \frac{(4\pi)^2}{Q^4} \sum_k \sum_{\ell=1,2,3} \left[\left(\frac{Z_\alpha \alpha_s}{4\pi} \right)^{\ell+1} A_k^{(\ell)} \otimes \langle \mathcal{O}_k \rangle^{(0)} \right],$$

$$\Pi_\mu = (p+p')_\mu \left[(e_u - e_d) \frac{4\pi\alpha_s}{Q^4} \sum_k T_k \otimes \langle \mathcal{O}_k \rangle \right]. \qquad (11)$$

- Comparing the above two expressions of Π_μ order-by-order, one obtain the master formulae up to NNLO

$$T_1^{(0)} = A_1^{(0)},$$

$$T_1^{(1)} = A_1^{(1)} + Z_\alpha^{(1)} A_1^{(0)} - \sum_{k=1,2} Z_{k1}^{(1)} \otimes T_k^{(0)},$$

$$T_1^{(2)} = A_1^{(2)} + 2\, Z_\alpha^{(1)} A_1^{(1)} + Z_\alpha^{(2)} A_1^{(0)} - \sum_{k=1,2,3} \sum_{\ell=1,2} Z_{k1}^{(\ell)} \otimes T_k^{(2-\ell)}, \qquad (12)$$

- Main tasks: $A_1^{(2)}$, $Z_{21}^{(2)}$.
- Z_{11} can be determined from ERBL kernels.
- Z_{21}, Z_{31} are determined by requiring the IR-finite matrix elements $\langle \mathcal{O}_{2,3} \rangle$ vanish (decouple from the physical operator).
- Renormalization schemes of the evanescent operators are typically non-minimal and thus contributes constant terms.

Computation of $A_1^{(2)}$

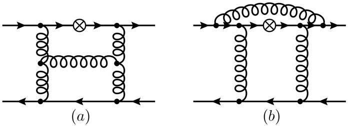

- The diagrams are generated by `FeynArts`, and there are 1066 diagrams contribute.

  1889(1602) diagrams generated in $n_f = 3(2)$.
- In reducing the tensor structure, we retained the operator structure.
- Target integrals are reduced with `FIRE` and 57 master integrls are solved by DEs.
- Canonical form is obtained with Lee's algorithm as implemented in the program `Libra`.

  R. N. Lee, JHEP 04, 108 (2015), arXiv:1411.0911 [hep-ph].

  R. N. Lee, Comput. Phys. Commun. 267, 108058(2021), arXiv:2012.00279 [hep-ph].
- Boundary condition is fixed using the PSLQ algorithm with 100 digits numerical results given by `AMFlow` at three distinct kinematic points.

  X. Liu and Y.-Q. Ma, Comput. Phys. Commun. 283,108565 (2023), arXiv:2201.11669 [hep-ph].

Computation of $Z_{21}^{(2)}$

- Similar to the 2-loop ERBL kernel calculation...

$$Z_{21}^{(2)} = -M_{21}^{\mathrm{off}(2)} + \sum_{j=1}^{3} M_{2j}^{\mathrm{off}(1)} \otimes M_{j1}^{\mathrm{off}(1)} \tag{13}$$

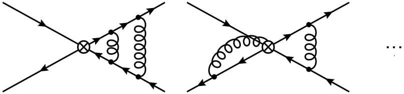

- 33 diagrams that exchange gluon between u- and d-quark contribute.
- δ-function generated by Wilson line Feynman rules is expressed as $\delta(x) = \mathrm{Disc}_x \frac{1}{x}$

$$\mathrm{Disc}_{x'} \int \frac{d^D l_1\, d^D l_2}{(i\pi^{D/2})^2} \frac{1}{[l_1^2 - m^2][l_2^2 - m^2][(l_1 + l_2 + x\, p)^2 - m^2][(l_1 + l_2 + p)^2 - m^2]} \frac{1}{n \cdot l_1 + x'} .$$

- Targets with linear propagators are reduced to about 30 master integrals.
- Master integrals are partly checked by `AMFlow`.
- Some diagrams are independently checked by evanescent mixing from $\gamma\gamma^* \to \pi^0$.

J. Gao, T. Huber, Y. Ji, and Y.-M. Wang, Phys. Rev. Lett. 128, 062003 (2022), arXiv:2106.01390 [hep-ph].

- $Z_{21}^{(2)}$ is independent of regulator m.

Expression of $T_1^{(2)}$

Collecting all pieces together results in a lengthy expression of $T_1^{(2)}$

$$
\begin{aligned}
T_1^{(2)} &= 1 \times \frac{1}{1-x} \times \frac{(C_A - 2C_F)C_F(540C_A\zeta_3 - 360C_F\zeta_3 + 630C_F\zeta_4)}{60N_c} \\
&+ G(0,x) \times \frac{1}{(1-x)(1-x-y)} \times \frac{(C_A - 2C_F)^2 C_F(-6\zeta_2 + 18\zeta_3)}{12N_c} \\
&+ G(0,y)G(1,x) \times \frac{1}{x^2(x-y)} \times \frac{(C_A - 2C_F)C_F(28n_\ell + 6C_F(51 + 6\zeta_2) + C_A(-301 + 54\zeta_2))}{36N_c} \\
&+ G(0,y)^3 \times \frac{1}{x(x-y)} \times \frac{C_F^3}{6N_c} \\
&+ G(0,x)G(1,1,y,x) \times \frac{1}{xy} \times \frac{C_F(-7C_A^2 + 3C_AC_F + 5C_F^2)}{N_c} + \dots,
\end{aligned}
$$

- About 3000 individual terms of the form

$$
\boxed{\mathrm{GPL} \times \frac{1}{x^{a_1} y^{a_2} (1-x)^{a_3} (1-y)^{a_4} (x-y)^{a_5} (1-x-y)^{a_6}} \times \mathrm{const}}
$$

- There exist unphysical poles in the result.
- When convoluted with $\phi_\pi^{\mathrm{Asy}}(x,\mu) = 6\,x\,(1-x)$, log divergences may appear in individual term.
- Multivariable partial fraction decomposition is used to simplify the results.

Scheme independence of form factor

$$F_\pi(Q^2) = (e_u - e_d)\frac{4\pi\alpha_s(\nu)}{Q^2} f_\pi^2 \int dx \int dy \, T_1(x, y, Q^2, \nu, \mu)\, \phi_\pi(x,\mu)\, \phi_\pi(y,\mu)\,,$$

- The leading-twist pion LCDA ϕ_π merely depends on the γ_5 scheme, so as T_1.
- For a change of evanescent basis

$$\boxed{\tilde{\mathcal{O}}_1 = \mathcal{O}_1, \qquad \tilde{\mathcal{O}}_2 = \mathcal{O}_2 + \kappa_2\,\epsilon\,\mathcal{O}_1, \qquad \tilde{\mathcal{O}}_3 = \mathcal{O}_3 + \kappa_3\,\epsilon\,\mathcal{O}_1}, \tag{14}$$

with an essential constraint $Z_{12} = Z_{13} = 0$, the "new" hard kernel leads to

$$\tilde{T}_1^{(\ell)} = T_1^{(\ell)} - \epsilon \sum_{n=2,3} \kappa_n\, T_n^{(\ell)}\,. \qquad (\ell = 0, 1, 2) \tag{15}$$

The finite hard kernels $T_{2,3}^{(\ell)}$ thus ensure the evanescent scheme independence of the hard kernel.

- For the case of $Z_{1n} \neq 0$, at NLO

$$\tilde{T}_1^{(1)} = T_1^{(\ell)} - \epsilon \sum_{n=2,3} \kappa_n\, T_n^{(\ell)} - \epsilon \sum_{n=2,3} \kappa_n Z_{1n}^{(1)} \otimes T_1^{(1)}\,. \tag{16}$$

The hard kernel exhibits scheme dependence, as is the case for the nucleon LCDA.

Y.-K. Huang, B.-X. Shi, Y.-M. Wang, and X.-C. Zhao, (2024), arXiv:2407.18724 [hep-ph].

Asymptotic form factor

Asymptotic pion LCDA

$$\phi_\pi^{\mathrm{Asy}}(x,\mu) = 6\,x\,(1-x), \tag{17}$$

Performing the two-fold convolution (with `PolyLogTools`) results in
C. Duhr and F. Dulat, JHEP 08, 135 (2019), arXiv:1904.07279 [hep-th].

$$\begin{aligned}
F_\pi^{\mathrm{Asy}}(Q^2) &= (e_u - e_d)\frac{4\pi\alpha_s(\nu)}{Q^2} 9 f_\pi^2 \left(\frac{C_F}{2N_c}\right)\left\{1 + \left(\frac{\alpha_s}{4\pi}\right)\left[\beta_0 \ln\frac{\nu^2}{Q^2} + \frac{14}{3}\beta_0 - \frac{71}{6}C_F + \frac{1}{3N_c}\right]\right.\\
&+ \left(\frac{\alpha_s}{4\pi}\right)^2\left[\left(\beta_1 \ln\frac{\nu^2}{Q^2} - \beta_0^2 \ln^2\frac{\nu^2}{Q^2}\right) + 2\beta_0\left(\beta_0\ln\frac{\nu^2}{Q^2} + \frac{14}{3}\beta_0 - \frac{71}{6}C_F + \frac{1}{3N_c}\right)\ln\frac{\nu^2}{Q^2}\right.\\
&\underline{+4\left(C_F\beta_0\left(\frac{5}{2} - \zeta_2\right) - 2C_F^2(\zeta_2+\zeta_3)\right)\ln\frac{\mu^2}{Q^2}} + C_A^2\left(\frac{34873}{81} + \frac{88}{3}\zeta_2 + \frac{152}{3}\zeta_3 - 160\zeta_5\right)\\
&- C_A C_F\left(\frac{8191}{18} + \frac{1163}{9}\zeta_2 + 418\zeta_3 - 2\zeta_4 - 760\zeta_5\right) + C_F^2\left(194 + 61\zeta_2 + 246\zeta_3 - 18\zeta_4 - 560\zeta_5\right)\\
&\left.\left.- C_A n_\ell T_F\left(\frac{21742}{81} + \frac{32}{3}\zeta_2 - 48\zeta_3 + \frac{160}{3}\zeta_5\right) + C_F n_\ell T_F\left(\frac{769}{9} + \frac{316}{9}\zeta_2 - 8\zeta_3\right) + (n_\ell T_F)^2\frac{3496}{81}\right]\right\},
\end{aligned} \tag{18}$$

- Harmonic number series

$$\left(\sum_{m'=0}^{\infty}\gamma_{m',0}^{(1)} + \sum_{n'=0}^{\infty}\gamma_{n',0}^{(1)}\right) = 4\left(C_F\beta_0\left(\frac{5}{2} - \zeta_2\right) - 2C_F^2(\zeta_2+\zeta_3)\right) \tag{19}$$

- $\phi_\pi^{\mathrm{Asy}}(x,\mu)$ is not eigenfunction of ERBL kernels beyond NLO.

Numerical analysis

- ϕ_π models needed to calculate $F_\pi(Q^2)$

$$F_\pi(Q^2) = (e_u - e_d)\frac{4\pi\alpha_s(\nu)}{Q^2} f_\pi^2 \int dx \int dy\, T_1(x, y, Q^2, \nu, \mu)\, \phi_\pi(x,\mu)\, \phi_\pi(y,\mu)\,, \tag{20}$$

- Expanding ϕ_π in Gegenbauer polynomials

$$\phi_\pi(x,\mu) = 6\,x\,(1-x) \sum_{m=0,2,4,\dots}^{\infty} a_m(\mu)\, C_m^{3/2}(2x-1)\,. \tag{21}$$

$$\text{Model I}: \phi_\pi(x,\mu_0) = \frac{\Gamma(2+2\alpha_\pi)}{\Gamma^2(1+\alpha_\pi)}(x\bar{x})^{\alpha_\pi}\,, \text{with } \alpha_\pi(\mu_0) = 0.585^{+0.061}_{-0.055}$$

S. J. Brodsky et al, Phys. Rev. D 77, 056007 (2008), arXiv:0707.3859 [hep-ph].

G. S. Bali et al, JHEP 08, 065 (2019), [Addendum: JHEP 11, 037 (2020)], arXiv:1903.08038 [hep-lat].

$$\text{Model II}: \{a_2, a_4, a_6, a_8\}(\mu_0) = \{0.181(32), 0.107(36), 0.073(50), 0.022(55)\}\,,$$

S. Cheng et al, Phys. Rev. D 102, 074022 (2020), arXiv:2007.05550 [hep-ph].

$$\text{Model III}: \{a_2, a_4\}(\mu_0) = \{0.149^{+0.052}_{-0.043}, -0.096^{+0.063}_{-0.058}\}\,,$$

N. G. Stefanis, Phys. Rev. D 102, 034022 (2020), arXiv:2006.10576 [hep-ph].

$$\text{Model IV}: \{a_2, a_4, a_6\}(\mu_0) = \{0.196(32), 0.085(26), 0.056(15)\}, \quad \mu_0 = 2\,\text{GeV}\,.$$

I. Cloet et al, arXiv:2407.00206 [hep-lat].

Numerical analysis

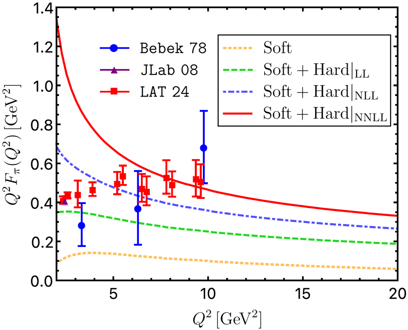

- Model-I as the default choice.
- $\nu^2 = Q^2,\ \mu^2 = 1/2Q^2$.
- NNLO correction: about $30\% \sim 50\%$ at $Q^2 \in [5, 20]\,\text{GeV}^2$.
- Soft contribution: about 25%.

Numerical analysis

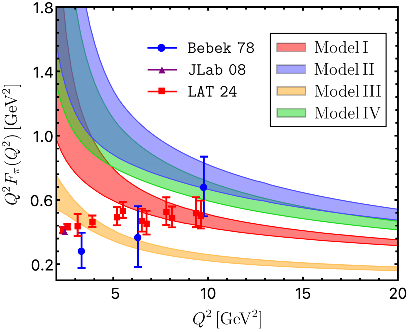

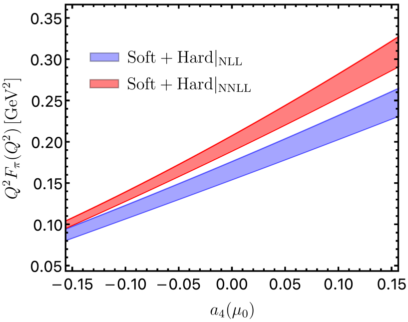

- Errors come from $\nu^2 \in [1/2, 2]\,Q^2,\ \mu^2 \in [1/4, 3/4]\,Q^2$.
- Well-separated bands $\Rightarrow$ Distinguishing different models.

- Errors come from $\nu^2 \in [1/2, 2]\,Q^2,\ \mu^2 \in [1/4, 3/4]\,Q^2$.
- $Q^2 = 30\,\mathrm{GeV}^2$, within the range of EIC (up to $40\,\mathrm{GeV}^2$).
- Higher sensitivity at NNLO.
- $a_{n\geq 6} = 0$.

Summary

- NNLO pion EMFF with modern effective field theory formalism rigorously.
  - Ideal hard exclusive process for QCD factorization.
  - Two-loop bare amplitude from standard multi-loop technology.
  - Non-trivial IR subtraction procedure due to evanescent operators.
  - Substantial two-loop numerical impact to pion EMFF.
  - Higher sensitivity for extracting the Gegenbauer moment a_4.
- Future studies
  - Inclusion of massive quark loops.
  - $B_c \to \eta_c \, \ell \, \bar{\nu}_\ell$ transition form factors.
  - ...

Thank you for your attention!